Investigations of the Equilibrium and Stability Behaviour of Tokamak Discharges in Pulsator I

O. Klüber

IPP III/14 August 1974

MAX-PLANCK-INSTITUT FÜR PLASMAPHYSIK

GARCHING BEI MÜNCHEN

MAX-PLANCK-INSTITUT FÜR PLASMAPHYSIK

GARCHING BEI MÜNCHEN

Investigations of the Equilibrium and Stability Behaviour of Tokamak Discharges in Pulsator I

O. Klüber

IPP III/14 August 1974

Die nachstehende Arbeit wurde im Rahmen des Vertrages zwischen dem Max-Planck-Institut für Plasmaphysik und der Europäischen Atomgemeinschaft über die Zusammenarbeit auf dem Gebiete der Plasmaphysik durchgeführt.

III/14 O. Klüber

Investigations of the Equilibrium and Stability Behaviour of Tokamak Discharges in Pulsator I

Abstract

This report briefly describes the Pulsator I tokamak and discusses some important properties of the plasmas produced in this apparatus, emphasis being placed on the equilibrium and stability behaviour. The experiments show two different forms of the disruptive instability, a "hard" and a "soft" type, which are clearly governed by the position of the plasma column before the onset of the instability, i. e. whether it is displaced inwards or outwards, respectively. The difference is explained in semi-phenomenological terms, the explanation being supported by definitive experiments. The use of programmed vertical fields allows good long-term centering of the plasma column and hence stable, reproducible discharges with q values down to 2.3. Finally, the time development of the mean electron density is discussed.

Contents

I. Description of the machine and operating conditions

The main parameters of Pulsator are:

Major radius	R	= 70 cm
Limiter radius	a	= 12 cm
Aspect ratio	A	= 5.83
Maximum toroidal magnetic field	B_φ	= 30 kG
Plasma current for q = 3	I	= 100 kA
Maximum pulse length		0.2 s

The machine is sketched in Fig. 1; its components are briefly described in the following.

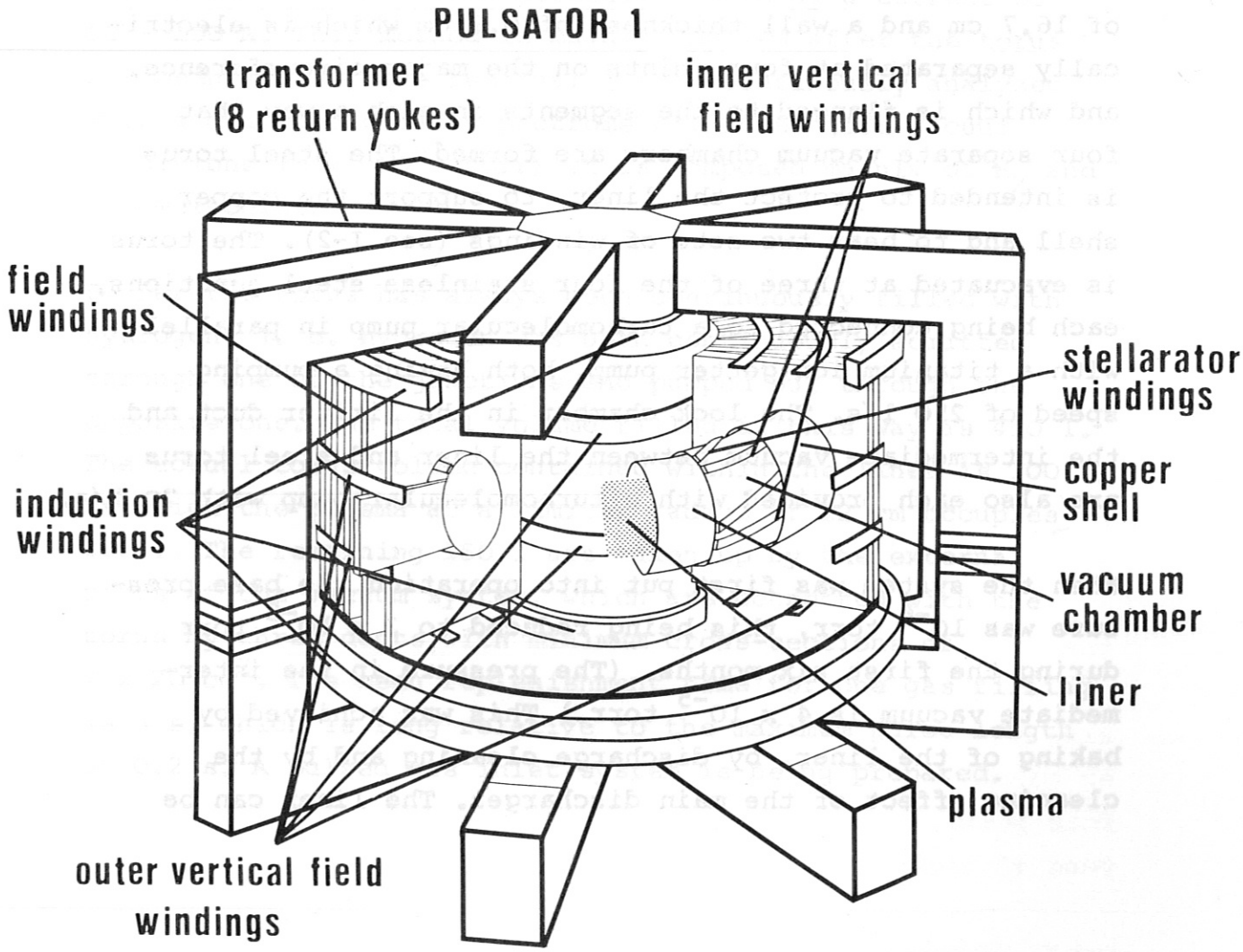

Fig. 1 Schematic view of Pulsator I

I-1 Discharge vessel and vacuum system

The liner consists of 0.3 mm thick stainless steel bellows with an inner radius of 14 cm, a corrugation depth of 1.6 cm and an ohmic resistance of 21 mΩ. It is interrupted at four points on the major circumference by solid stainless steel segments with a minimum inner radius of 13 cm to which the quadrants of the liner are flanged. These segments are fitted with ports which are used for evacuation, diagnostics and installing the limiter. The duct through which the limiter is introduced is provided with a vacuum lock to allow the limiter to be replaced without having to vent the torus. The types of limiters used will be dealt with later. The liner is enclosed by a steel torus with an inner radius of 16.7 cm and a wall thickness of 0.8 cm which is electrically separated at four points on the major circumference, and which is flanged to the segments in such a way that four separate vacuum chambers are formed. The steel torus is intended to protect the liner, to support the copper shell and to bear two sets of windings (see I-2). The torus is evacuated at three of the four stainless steel junctions, each being connected to a turbomolecular pump in parallel with a titanium ion getter pump, both having a pumping speed of 250 l/s. The lock chamber in the limiter duct and the intermediate vacuum between the liner and steel torus are also each provided with a turbomolecular pump with 70 l/s.

When the system was first put into operation the base pressure was 10^{-6} torr, this being reduced to 3×10^{-8} torr during the first six months. (The pressure in the intermediate vacuum is 4×10^{-5} torr.) This was achieved by baking of the liner, by discharge cleaning and by the cleaning effect of the main discharges. The liner can be

baked to a maximum of 200°C by an induced alternating current. The outer steel torus and the junctions thereby assume a temperature of 70°C as a result of heat transfer from the liner and the external parts of the vacuum system, which are additionally baked with strip heaters. For the discharge cleaning use is made of part of the OH system (see I-3), which generates 60 kA current pulses of 1 ms length at a repetition rate of one every 4 s. Before the start of a series of measurements it is customary to perform 600 - 1000 such discharges. Cleaning discharges can also be produced by means of induced alternating currents with a typical value of 200 A at 50 Hz. Under these conditions the resistance of the liner is not much higher than that of the plasma, and so it is in addition directly heated by a current of 50 - 100 A. This method is mainly applied after the torus has been vented. The residual gas is continously analyzed with a quadrupole mass spectrometer. Under good vacuum conditions ($p < 10^{-7}$ torr) it is composed mainly of H_2 and H_2O molecules.

So far the torus has always been continuously filled with hydrogen, i. e. hydrogen has been continuously admitted through one of the junctions and pumped out through the opposite one. The total volume filled in this way is 450 l. The actual torus volume contained within the liner is 300 l, of which the plasma at a limiter radius of 12 cm occupies 200 l. The remaining 150 l are taken up by the external parts of the vacuum system, which are connected with the torus by three ducts with minimum cross-sections of 2×20 cm^2. The mean replenishment time for one gas filling is 3 s, which is long relative to the maximum pulse length of 0.2 s. A pulsed gas inlet system is being prepared.

I-2 Magnetic field systems

The toroidal magnetic field of 30 kG maximum is produced with 48 water-cooled Bitter coils. The geometric ripple at the plasma surface is 0.2 %. The power source is a 14 MJ - 19 MW flywheel generator - transformer - rectifier - assembly with a flat-top time of 0.2 s maximum. The matching of the apparatus to this relatively small generator was a stringent boundary condition on the design of Pulsator I.

The magnetic field produced by the main field coil assembly was measured with an electron beam[1]. It was found that the field lines did not close. This can be explained as the superposition of two distinct fields on the toroidal field B_φ-- a vertical field, $B_z = 1.2 \times 10^{-3} B_\varphi$ (i. e. 36 G at 30 kG), and a radial field which is on the average a factor of 6 weaker than B_z, but which is not proportional to B_φ, depending instead on the magnetization state of the iron core. These stray fields are due partly to deviations of the field coils from their ideal positions and partly to the fact that the connections and return leads of the field coils are not located in the midplane.

The current directions for the main field coil current and plasma current were chosen such that the above-mentioned vertical stray field results in an inward displacement of the plasma column; the radial field then leads to a slight upward displacement. The radial stray field of the primary circuit which is produced by the asymmetry of the transformer core (the upper yoke branch can be removed; hence the slits there are larger than below) also acts in the same direction (see I-3). The radial field can be corrected by correcting windings (which are not shown in Fig. 1). This possibility, however, was only resorted to in the case of high-current discharges ($I > 100$ kA).

---

1) These measurements were made by R. Aymar and D. Eckhartt.

The vertical field required to achieve tokamak equilibrium is made up of three components:

a) First there is a copper shell with an inner radius of 19.5 cm and a wall thickness of 2.5 cm. It has a slit running toroidally in the midplane and four poloidal slits of only 3 mm width which are each displaced 45° to the junctions. Larger openings are caused by the pump and diagnostic ports. The perturbations of rotational symmetry caused by these openings were taken into account in determining the equilibrium position of the plasma.

b) The eight conductors fitted outside the main field coil assembly, the so-called external vertical field windings, whose spatial layout is shown in Fig. 1, can produce a stationary vertical field of 160 G maximum. The current is produced by a small pulse generator with a pulse length of a few seconds and is always switched on in such a way that the vertical magnetic field has completely penetrated the copper shell before the start of the plasma discharge. This also applies to the above-mentioned vertical stray field of the main field coil assembly, this field being added to the external vertical field.

c) On the outside of the steel torus, i. e. inside the copper shell, there are four toroidally aligned, series-connected conductors, the so-called inner vertical field windings, each at 45° to the midplane. These are used for producing programmed vertical fields or, to be more precise, for producing vertical fields by means of programmed currents. Of course, for the time development of the fields the currents induced in the copper shell have to be taken into account. They decay with a time constant of 60 ms.

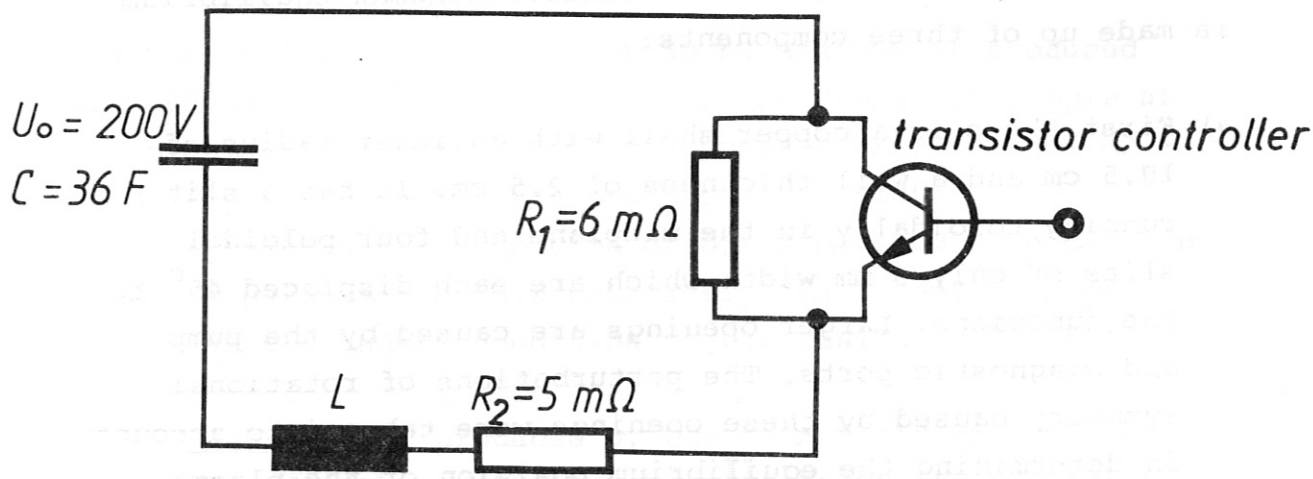

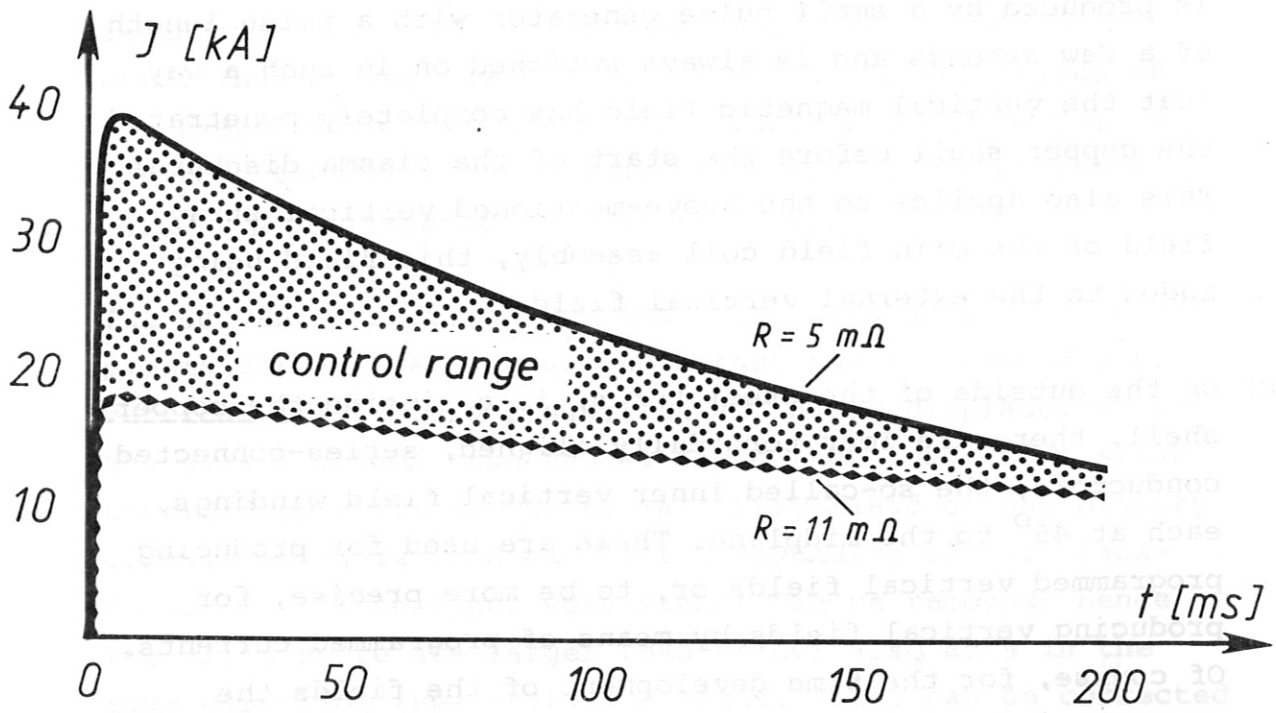

Fig. 2 Block diagram and current range of the power supply for the inner vertical field windings.

A schematic of the power supply is shown in Fig. 2. The capacitor bank (C = 36 F, $CU^2/2$ = 720 kJ) together with the resistors $R_1 + R_2$ (R_2 contains the ohmic resistance of the vertical field windings) and the inductance L of the windings forms a strongly damped oscillating circuit. Parallel to R_1 is a set of transistors which can be operated to vary the total resistance R between R_2 and $R_1 + R_2$. The time development of the current for the limiting cases $R = R_2$ and $R = R_1 + R_2$ is also shown in Fig. 2; the hatched region between the two curves is thus the range of adjustment. Adjustment is made over 200 ms on 20 channels whose length increases exponentially from 4 ms to 15 ms.

On the outside of the steel torus there is also a stellarator winding with two pairs of conductors on the minor circumference and one field period on the major circumference. It can also be powered by the above described, transistor-controlled capacitor bank. The rotational transform attainable at full current and maximum main magnetic field after the currents induced in the copper shell have decayed is $\iota/2\pi = 0.05$. The stellarator winding serves two purposes:

- production of an equilibrium configuration for a current-free preionization plasma
- investigation of the influence of a superimposed stellarator field on a tokamak plasma.

Experiments with the stellarator windings will be reported elsewhere.

I-3 OH system

The plasma current is induced by an iron-core transformer with eight return yokes. The position of the primary windings can be seen in Fig. 1. There are eight windings at the top and bottom of the center core, and four at the top and bottom near the return yokes. The windings are arranged in such a way that the stray field in the plasma region is small.

The power supply is a power crowbar system consisting of two primary capacitor banks (25 kV, 0.5 mF, 150 kJ and 7.5 kV, 3.2 mF, 90 kJ) either of which can be used to produce the current rise (rise times 1.2 and 3 ms respectively), and a system of 36 artificial delay lines with a total energy content of 235 kJ which can be connected in series or parallel in batches. The pulse length is about 0.2 s; it depends on the current, just as does the characteristic impedance, because iron chokes are used. By varying the voltage ratio between the primary bank and the delay lines it is possible to select various current programs. If the voltage of the primary bank is not sufficient to ignite the discharge, it is possible to precede it with an additional small high-voltage capacitor with a pulse length of about 0.1 ms.

II. Diagnostic methods

This section briefly describes the diagnostic methods used to obtain the results presented below.

- Two Rogowski coils are available for measuring the plasma current. One is located in a recess in one of the four junctions, the second in the intermediate vacuum chamber between the liner and the outer steel torus.

- Two Rogowski coils arranged in the same way are sub-divided into 8 and 12 sections respectively. The appropriate sections are used for determining the horizontal and vertical displacement of the plasma column. All sections may be used as magnetic probes. In addition there are many magnetic probes distributed around the torus in the midplane.

- The loop voltage can be picked up by test loops on the outside of the outer vacuum vessel.

- The electron density is measured with an 8-channel microwave interferometer. One channel is located in the midplane of the torus, the others being arranged in the vertical direction so that the whole plasma cross-section is covered. The interferometer, in its present version, may be operated at a wavelength $\lambda = 3.3$ mm or 2 mm. At a later stage it will be possible to have simultaneous operation with both wavelengths. The interferometer is described in detail in /1/.

- The electron temperature is determined by Thomson scattering. The light source, a ruby laser, and the optical system for gathering the scattered light are arranged so that the plasma can be scanned both vertically and horizontally. It is thus possible to cover almost the entire plasma cross-section. A more detailed description can be found in /2/.

The following methods were not used until later in the experiments and yielded results for some of the discharges described in section IV:

- measurement of the diamagnetic signal
- measurement of the X-radiation by PHA and the filter method
- measurement of the ion temperature by the charge exchange method.

Preparations are also being made for determination of the ionization rate from the emission of H_α (particle confinement time) and for spectroscopic measurements in the visible, quartz UV and vacuum UV.

III. Discharges with stationary vertical field

Pulsator I was first operated with only stationary vertical fields since the power supply for the programmed vertical field was available later than the other components. The initial phase provided a basis of comparison for the improvements possible with the programmed fields. This stage was characterized also by the successive application of various diagnostic methods. The discharge current I, the loop voltage U, the horizontal plasma displacement Δ and $\beta_p + l_i/2$ from the signal of the magnetic probes were measured from the outset; later the electron density was measured with the microwave interferometer and the electron temperature by Thomson scattering.

The tokamak plasmas produced with stationary vertical fields can be roughly described by the following data:

- plasma current $I \leq 60$ kA
- pulse length $t \leq 80$ ms
- inverse rotational transform $q \geq 4$
- stationary vertical field $B_z \leq 105$ G
- filling pressure $p_f = 0.4 - 2 \times 10^{-4}$ torr
- mean electron density $n_e = 1.5 - 4 \times 10^{13}$ cm^{-3}
- electron temperature $kT_e \leq 1.4$ keV.

In the following the equilibrium and stability behaviour of the discharge are the principal points of discussion. Figure 3 shows the equilibrium diagram for Pulsator I that is yielded by the well-known Shafranov equation

$$\Delta = \frac{b^2}{2R}\left[\ln\frac{b}{a} + \left(1-\frac{a^2}{b^2}\right)\left(\beta_p + \frac{l_i - 1}{2}\right)\right] - \Delta_B \quad ;$$

$$\Delta_B = \frac{2\pi b^2 B_z}{\mu_o I}$$

with the additional assumption $a = a_L - |\Delta|$ /3/, where a_L is the limiter radius. Positive Δ denotes, as usual, outward displacement. All other quantities have the standard meaning. In keeping with the experimental results, a value of 1.25 was substituted for $\beta_p + l_i/2$. Figure 3 clearly shows

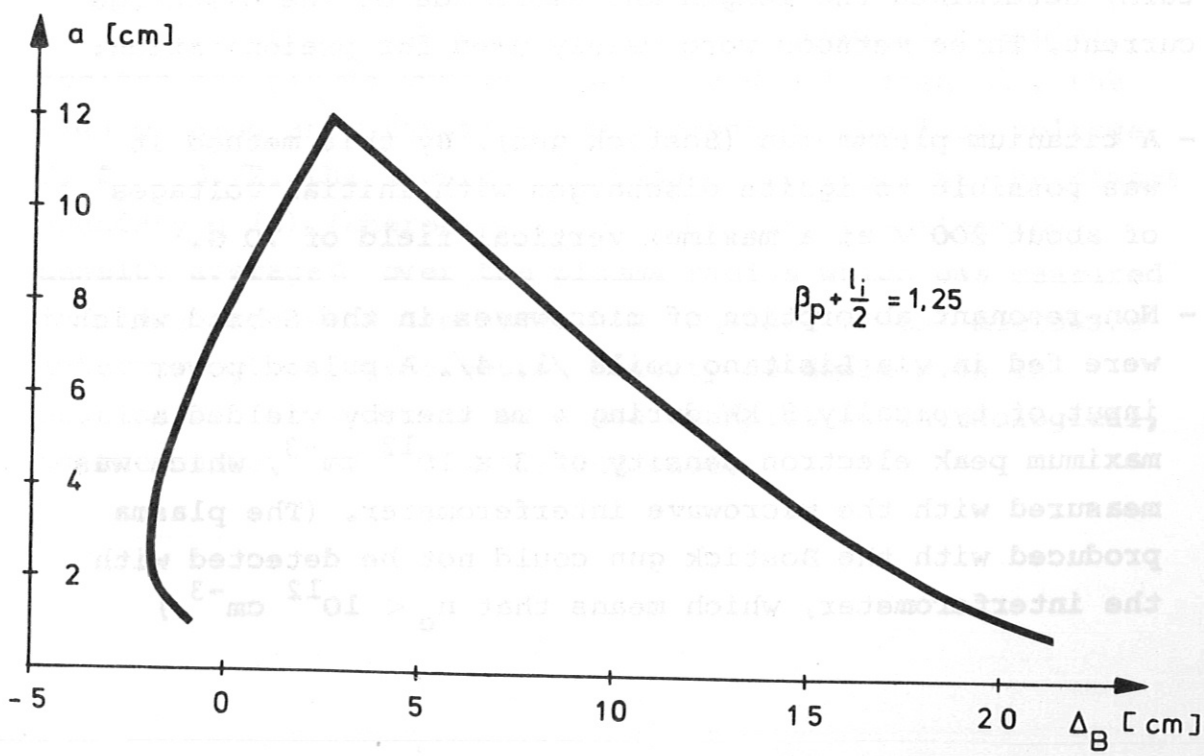

Fig. 3 Equilibrium diagram for Pulsator I

that without an external vertical magnetic field the plasma in Pulsator I would undergo very strong outward displacement. This is mainly due to the relatively large ratio $b/a_L = 19.5/12 = 1.63$ (cf. 1.27 in ST), which results from the double vacuum system and from the installation of the windings on the outer vacuum vessel. According to Figure 3 to center a plasma carrying a current of 60 kA, a vertical field of 81 G is necessary. (By comparison, equilibrium without a copper shell under otherwise equal conditions would require a vertical field of 330 G.)

As is well known, the ignition of tokamak discharges in stationary vertical fields of this strength presents difficulties because the plasma is then very strongly displaced inwards in the initial phase when the current is still low. Great value was therefore placed on good preionization from the outset. In fact, the maximum vertical field B_z at which the discharge could still be ignited was governed by the quality of the preionization. The vertical field, in turn, determined the length and amplitude of the discharge current. Three methods were mainly used for preionization:

- A titanium plasma gun (Bostick gun). By this method it was possible to ignite discharges with initial voltages of about 200 V at a maximum vertical field of 70 G.

- Non-resonant absorption of microwaves in the S-band which were fed in via Lisitano coils /1, 4/. A pulsed power input of typically 8 kW during 4 ms thereby yielded a maximum peak electron density of 3×10^{12} cm^{-3}, which was measured with the microwave interferometer. (The plasma produced with the Bostick gun could not be detected with the interferometer, which means that $n_e < 10^{12}$ cm^{-3}.)

- As the plasma production with Lisitano coils alone was restricted to a very narrow pressure range which was dependent on the vacuum conditions, mostly a combination of the two above-mentioned preionization methods was used, which allowed reliable ignition in the initial pressure range 0.4 - 2 x 10^{-4} torr and at a vertical field of up to 105 G.

The following should be added about the operating conditions:

- No premagnetization of the iron core
- No correction of the radial stray field
- In all discharges a standard type of limiter was used, namely a circular stainless steel disc to whose inner edge molybdenum or tungsten segments measuring 2 x 1 x 1 cm^3 are screwed.

The time development of the plasma current was essentially governed by that of the plasma displacement Δ ; the discharges shown in Figures 4, 5 and 6 are typical examples. Besides the plasma current I and the displacement Δ , the figures also show the time development of the loop voltage U, $\beta_p + l_i/2$, the inverse rotational transform at the plasma boundary q (a) (where $a = a_L - |\Delta|$), and the electron density averaged over the plasma radius which was measured in every case with the horizontal channel of the microwave interferometer. The electron density is dealt with in Section V. The sequence of these examples is chronological, as the numbers of the shots indicate.

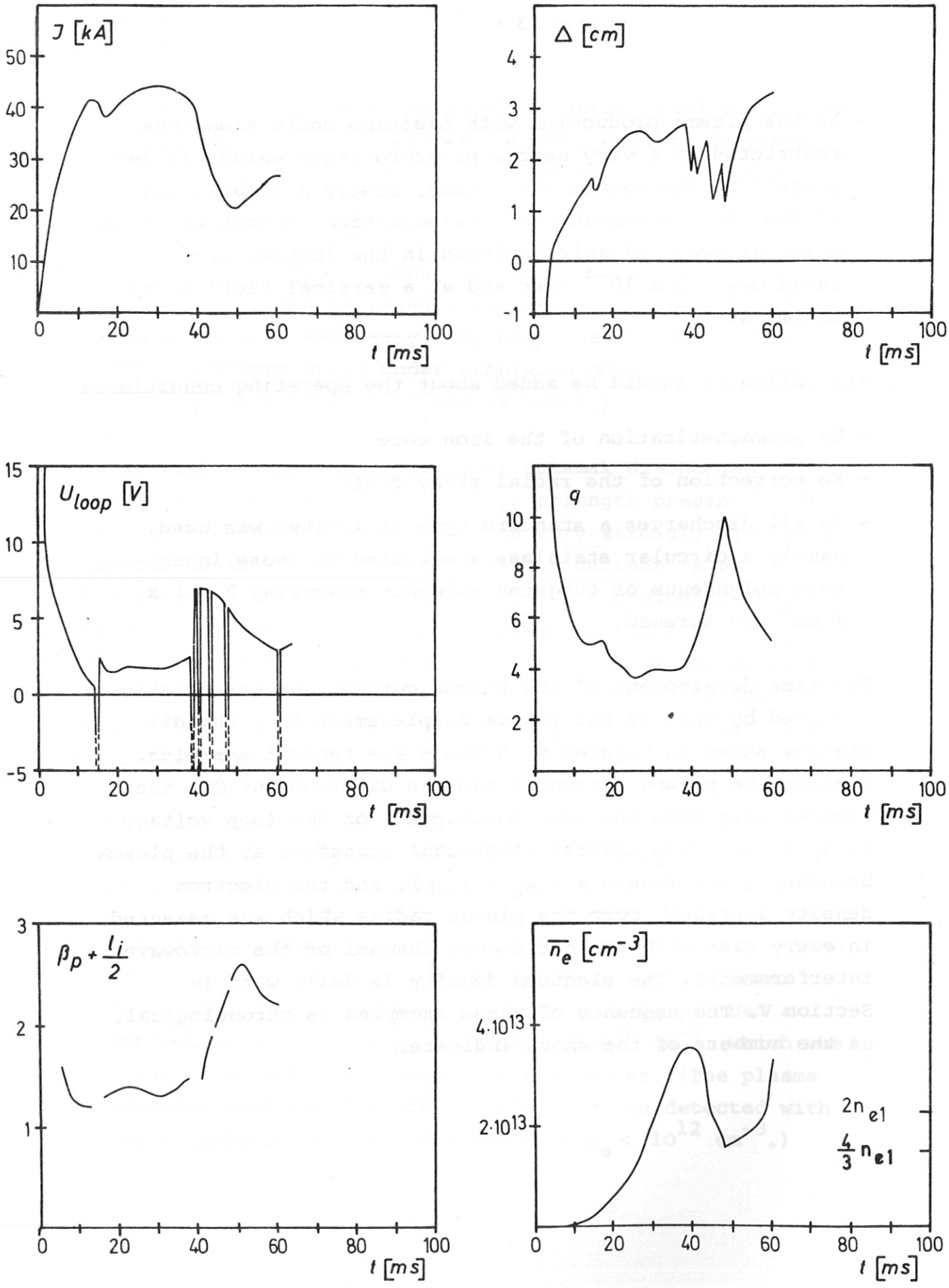

Fig.4. Shot No.712. Stationary vertical field B_z = 60 G. B_g = 26 kG.

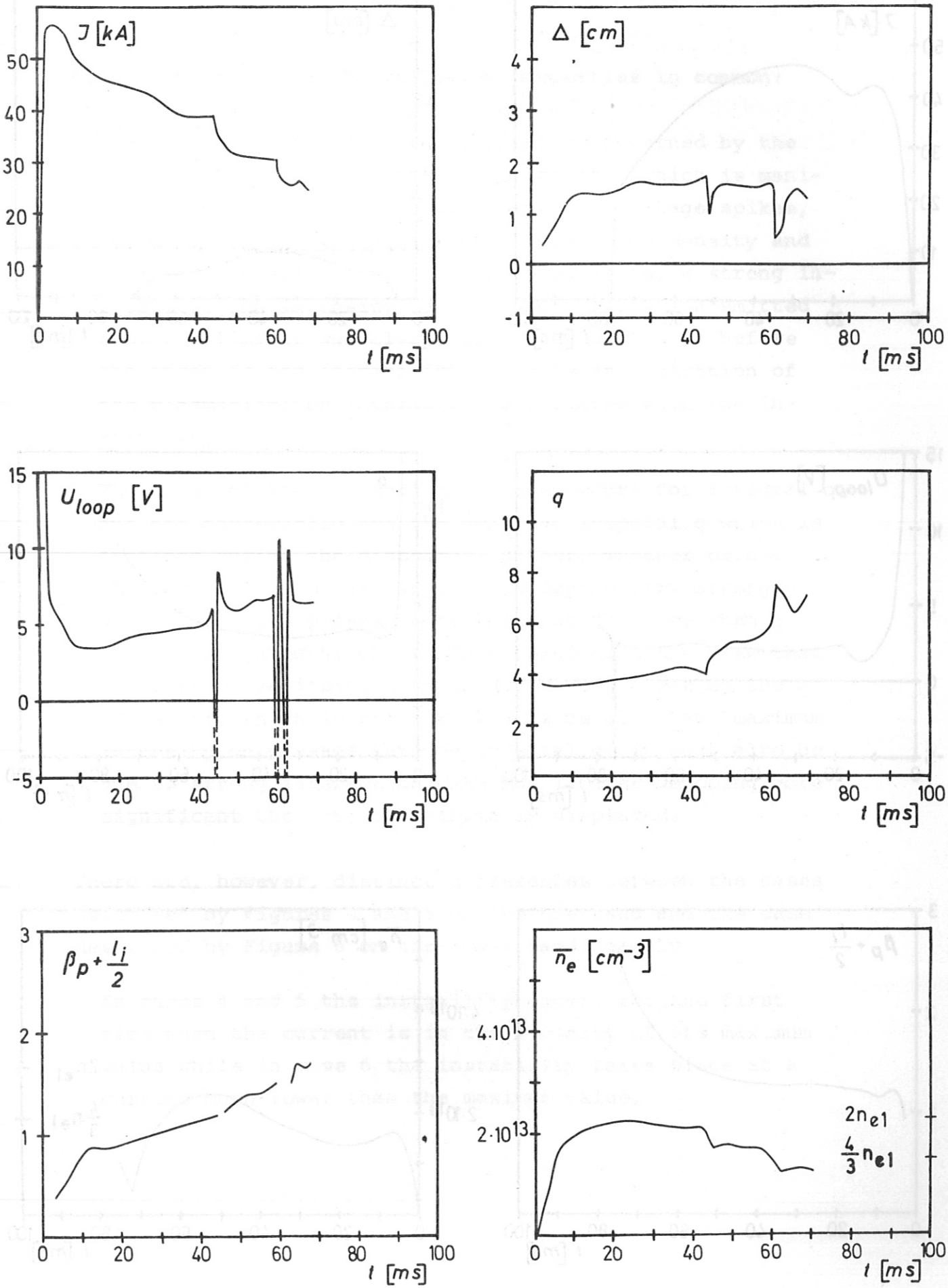

Fig.5. Shot No.834. Stationary vertical field B_z = 62 G. B_φ = 22kG.

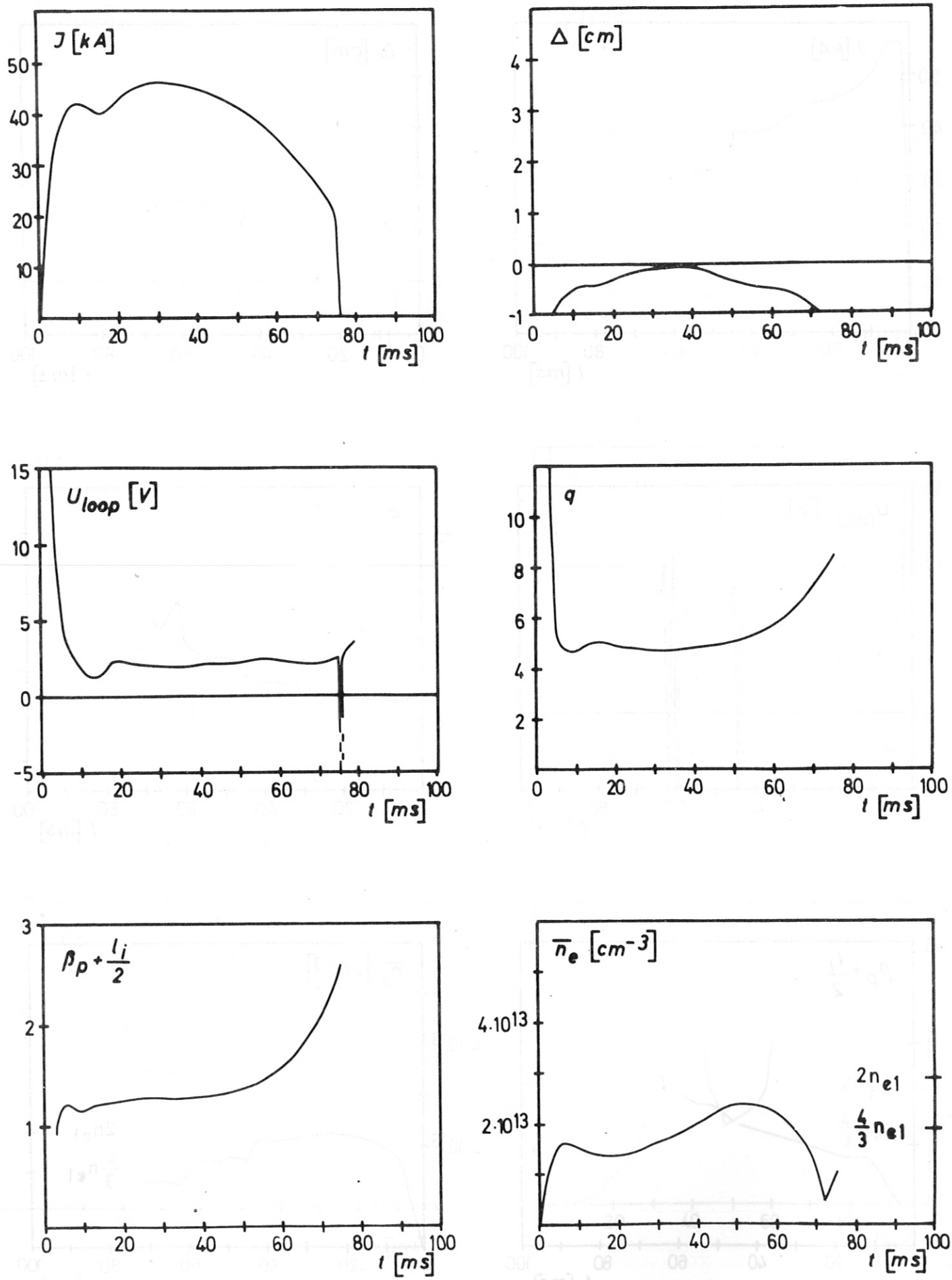

Fig.6. Shot No.1038. Stationary vertical field B_z = 105 G. B_φ = 22 kG.

All discharges have the following properties in common:

- The time development of the current is governed by the occurrence of the disruptive instability, which is manifested in the familiar manner: negative voltage spikes, decrease of the plasma current and electron density and an inward "displacement spike". In addition, a strong increase of the intensity of the hard X-radiation emitted from the limiter was always observed about 1 ms before the onset of the instability; this is an indication of the plasma-limiter interaction associated with the instability.

- The onset of the instability always occurs for integral q, but not necessarily for the smallest integral q which is attained during the discharge. Rather, whether or not the instability occurs appears to depend very strongly on how well the plasma is centered at the time when q assumes an integral value. This reinforces the view that the disruptive instability is not caused alone by the MHD modes, which in tokamak plasmas usually have maximum intensity on passage through integral q; it must also be due to strong interaction with the limiter becoming more significant the more the plasma is displaced.

There are, however, distinct differences between the cases described by Figures 4 and 5 on the one hand and the case described by Figure 6 on the other hand, namely

- In cases 4 and 5 the instability occurs for the first time when the current is in the vicinity of its maximum value while in case 6 the instability takes place at a current much lower than the maximum value.

- In cases 4 and 5 the instability first occurs when the plasma is strongly displaced outwards, while in case 6 the plasma is shifted inward at the time of the onset of the instability, the inward displacement increasing towards the end of the current pulse.

- In cases 4 and 5 the time constant with which the current decreases after the onset of the disruptive instability is much larger than in case 6.

Accordingly, a distinction has to be made between two forms of the disruptive instability, a "hard" and a "soft" type. The "soft" type occurs when the displacement is positive and increasing with time, the "hard" type when Δ is negative and decreasing with time. A simple explanation is afforded by the equilibrium diagram presented in Figure 3, taking into account the empirical results that the instability itself produces a shift of the plasma inwards and that the instability always results in a decrease of the current, even though very slight.

If the plasma is displaced outwards before the onset of the instability, the instability itself and the current decrease cause a reduction of the displacement, i. e. better centering of the plasma column and hence separation from the limiter. The plasma is then able to recover. Comparison of cases 4 and 5 shows that the current decrease is less the better the plasma was centered before the onset of the instability: In the case of Figure 4 the current decrease after the first instability at $q = 5$ is small. The current increases again until $q = 4$ is reached. Some time later the plasma becomes unstable. A series of instabilities reduces the current such that a further stable phase with increasing current follows. In the case of Figure 5 the plasma is better centered. The sequence of instabilities altogether causes only a slow decrease of the current.

If the plasma was already displaced inwards before onset of the instability, matters take a completely different course. In this case, according to Figure 3, both the instability itself and the current decrease associated with it lead to an increasingly strong inward displacement. This explains the rapid drop of the plasma current in case 6. In anticipation of the discharges with programmed vertical field that are treated in the next section it should be mentioned here that even though the plasma parameters are different under these conditions (e. g. smaller q) the instability depends on the displacement in the same way.

According to the foregoing, the plasma should be least sensitive to disruptive instabilites when it is well centered, but still slightly displaced outwards. This is largely confirmed by the experiments. In case 6 the plasma is always slightly displaced inwards. It should be borne in mind, however, that the determination of the plasma position from the signal of the magnetic probes may contain small errors. In particular, the magnetic surfaces are assumed to be circular; changes in shape such as are caused by vertical displacement are not taken into account. Furthermore, this method only determines the location of the current center. Determination of the interaction with the limiter certainly calls for more details, e. g. knowledge of the density and temperature gradients in the outer regions of the plasma column. Better agreement with the experiment is therefore not to be expected.

Nevertheless it can be stated that the displacement of the current center measured with the magnetic probes is also accompanied by a corresponding displacement of the density maximum. An example is shown in Figure 7, in which the time

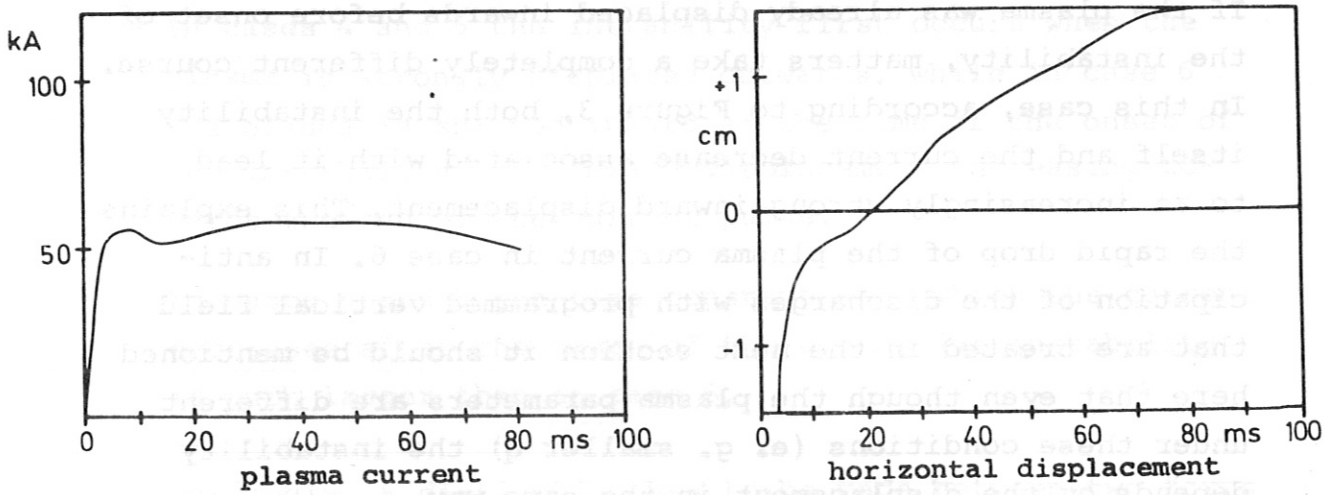

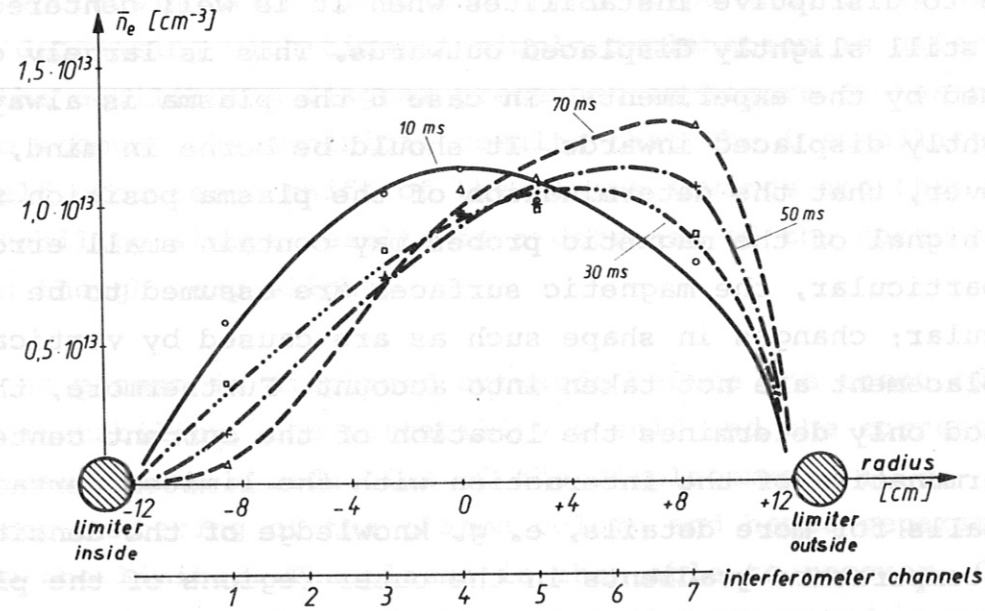

Fig. 7 Shot No. 939. Stationary vertical field B_z = 100 G. B_ϕ = 22 kG. Current, displacement and profiles of the electron density averaged over the microwave path lengths, these lengths being calculated under the assumption that the plasma boundary is a circle with the radius $a_L - |\Delta|$, centered at Δ.

development of I and Δ and the density profiles for several points in time are plotted for one discharge. Here $\bar{n}_e$ is the electron density averaged over the respective vertical chord length irradiated by the microwave interferometer. As Figure 7 shows, the density maximum is even more strongly displaced than the current center; the density distribution may thus deviate very strongly from rotational symmetry about the minor torus axis. The same applies to the electron temperature profiles.

IV. Discharges with programmed vertical fields

The experiments with stationary vertical fields clearly demonstrated the importance of the centering of the plasma column for achieving high-current discharges with long-term stability. With programmed vertical fields it was possible to center the plasma column much better for longer times thereby allowing the parameter range to be greatly extended as follows:

- plasma current $I \leq 125$ kA
- pulse length $t_I \leq 180$ ms
- inverse rotational transform $q \geq 2.3$

This yields a factor of 2 improvement as comparison with the data given at the beginning of Section III shows. The filling pressure was again varied in the same range, the mean electron density was between 3 and 6 x 10^{13} cm^{-3}, and the maximum electron temperature of 1.6 keV was insignificantly higher.

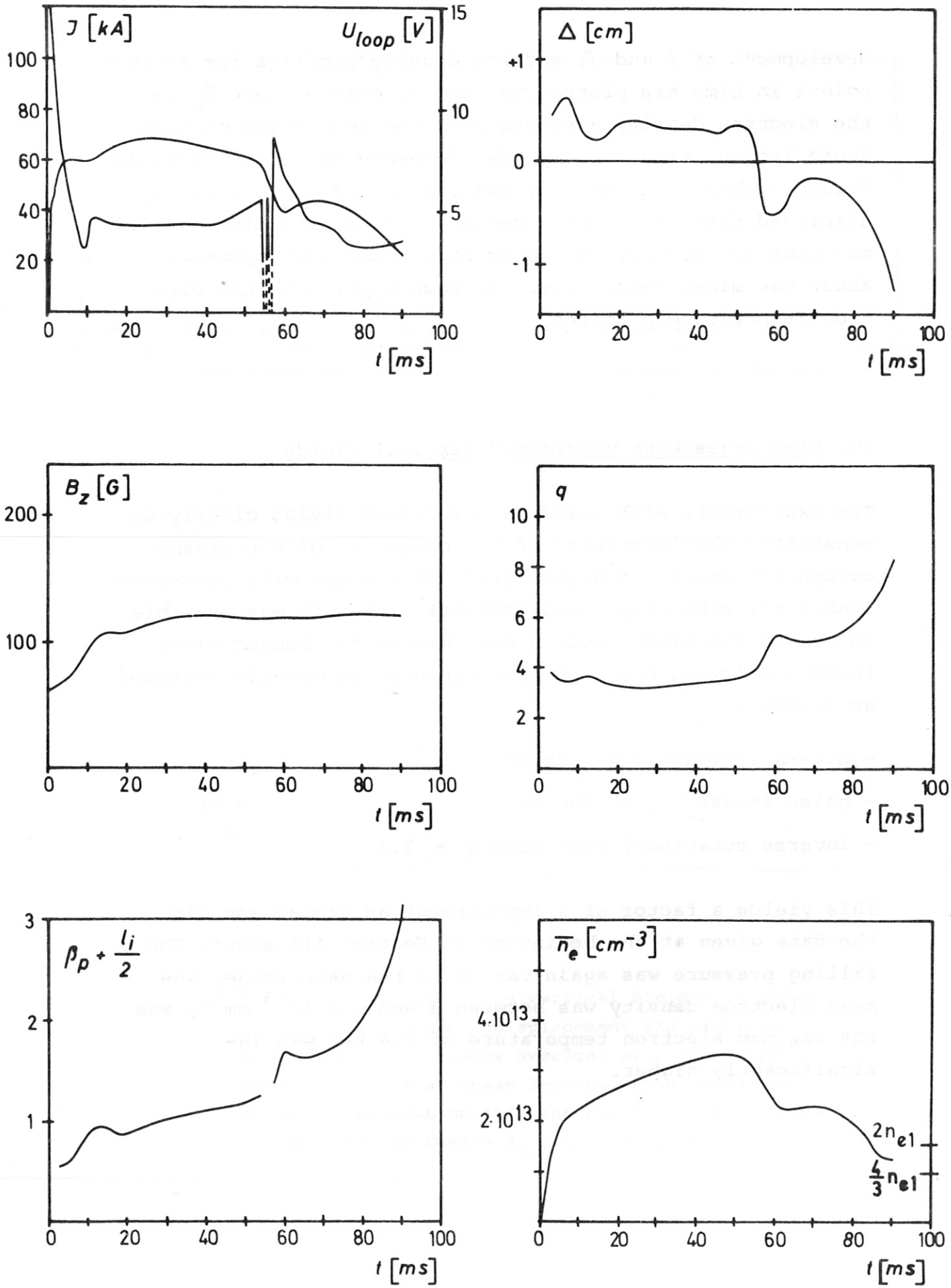

Fig.8. Shot No.1071. Programmed vertical field, B_φ = 22 kG.

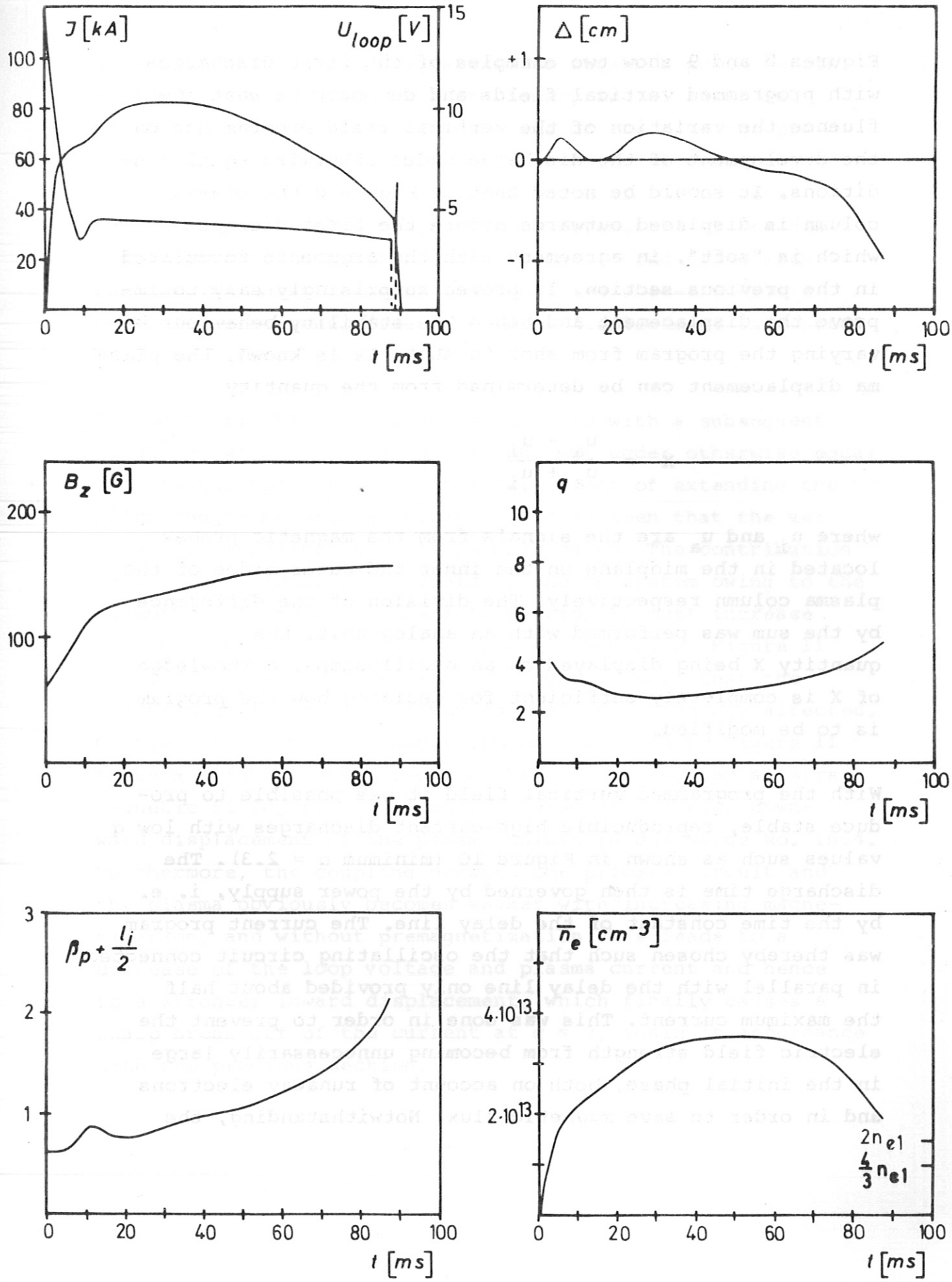

Fig.9. Shot No.1079. Programmed vertical field. B_φ = 22 kG.

Figures 8 and 9 show two examples of the first discharges with programmed vertical fields and demonstrate what influence the variation of the vertical field program has on the development of the discharge under otherwise equal conditions. It should be noted that in Figure 8 the plasma column is displaced outwards before the first disruption, which is "soft", in agreement with the arguments formulated in the previous section. It proved surprisingly easy to improve the displacement and hence the stability behaviour by varying the program from shot to shot. As is known, the plasma displacement can be determined from the quantity

$$X = \frac{u_a - u_i}{u_a + u_i}$$

where u_i and u_a are the signals from the magnetic probes located in the midplane on the inner and outer sides of the plasma column respectively. The division of the difference by the sum was performed with an analog unit, the quantity X being displayed on an oscilloscope. A knowledge of X is completely sufficient for deciding how the program is to be modified.

With the programmed vertical field it was possible to produce stable, reproducible high-current discharges with low q values such as shown in Figure 10 (minimum $q = 2.3$). The discharge time is then governed by the power supply, i. e. by the time constant of the delay line. The current program was thereby chosen such that the oscillating circuit connected in parallel with the delay line only provided about half the maximum current. This was done in order to prevent the electric field strength from becoming unnecessarily large in the initial phase, both on account of runaway electrons and in order to save magnetic flux. Notwithstanding, the

iron core had to be premagnetized to attain a pulse length of 180 ms. In addition, the stationary radial stray magnetic field was compensated by means of the windings provided for that purpose.This leads to vertical centering of the plasma column for the entire length of the current pulse, as Figure 11 shows, in which parameters of the discharge treated in Figure 10 are again plotted along with the vertical displacement Δ_z. Positive values indicate upward displacement. (The horizontal displacement is denoted by Δ as before.)

In Figure 11 this discharge is compared with a subsequent discharge without premagnetization, but under otherwise equal conditions. Apart from the trivial effect of extending the pulse length by premagnetization, it is seen that the vertical displacement is small in both cases. The contribution made to the radial stray field by the OH system owing to the asymmetry of the iron core (cf. Section I) must increase with the start of saturation, but it cannot, as Figure 11 shows, penetrate so fast into the copper shell that the position of the plasma column is thereby noticeably affected. On the other hand, premagnetization according to Figure 11 makes a slight contribution to the stationary, radial stray magnetic field, thus causing the somewhat stronger downward displacement of the plasma column in discharge No. 1654. Furthermore, the coupling between the primary circuit and the plasma obviously becomes weaker with increasing magnetization, and without premagnetization this leads to a decrease of the loop voltage and plasma current and hence to a stronger inward displacement, which finally causes a sharp break-off of the current at $q = 3$, again in accordance with the previous section.

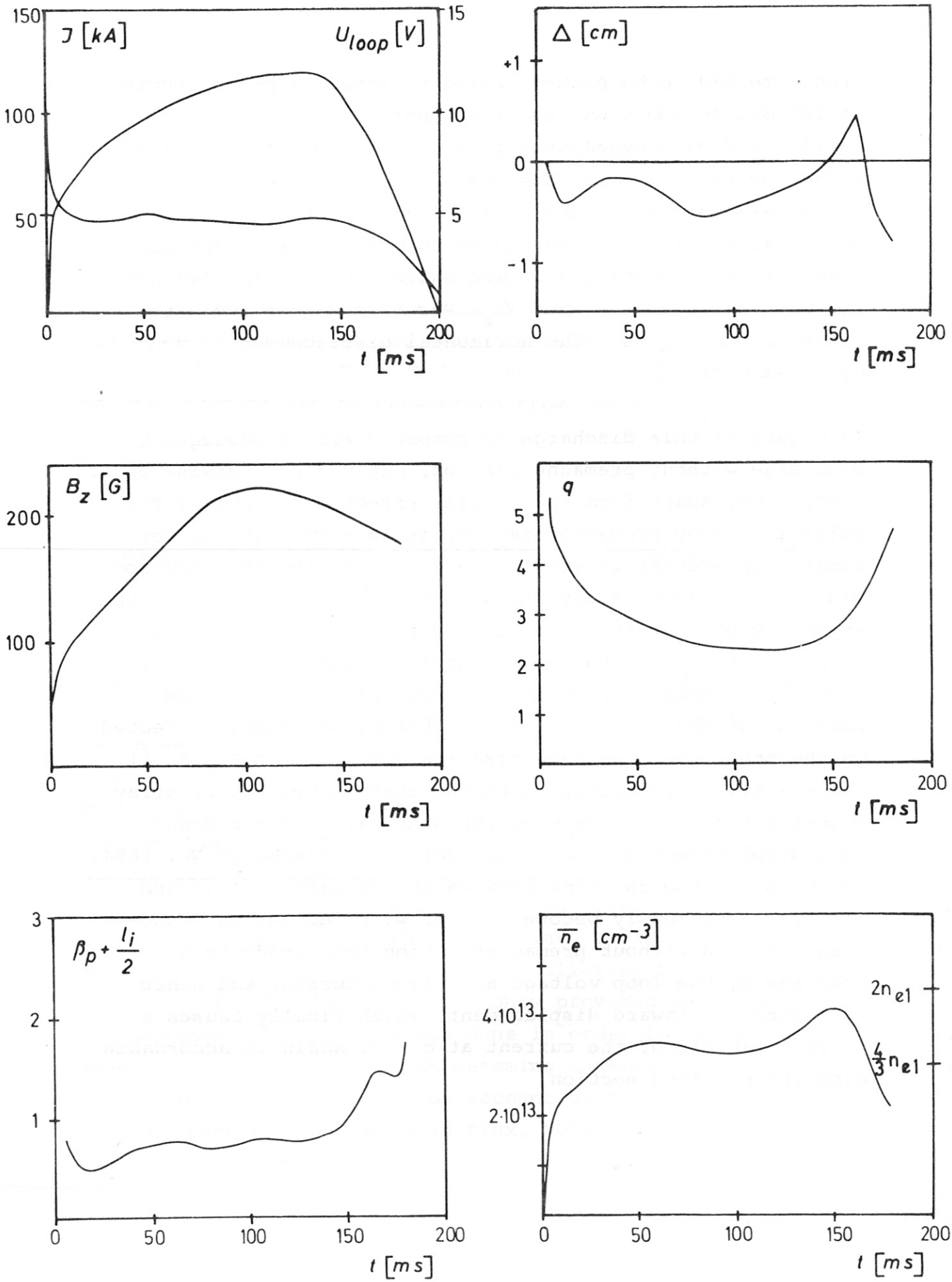

Fig.10. Shot No.1654. Programmed vertical field. B_φ = 28 kG.

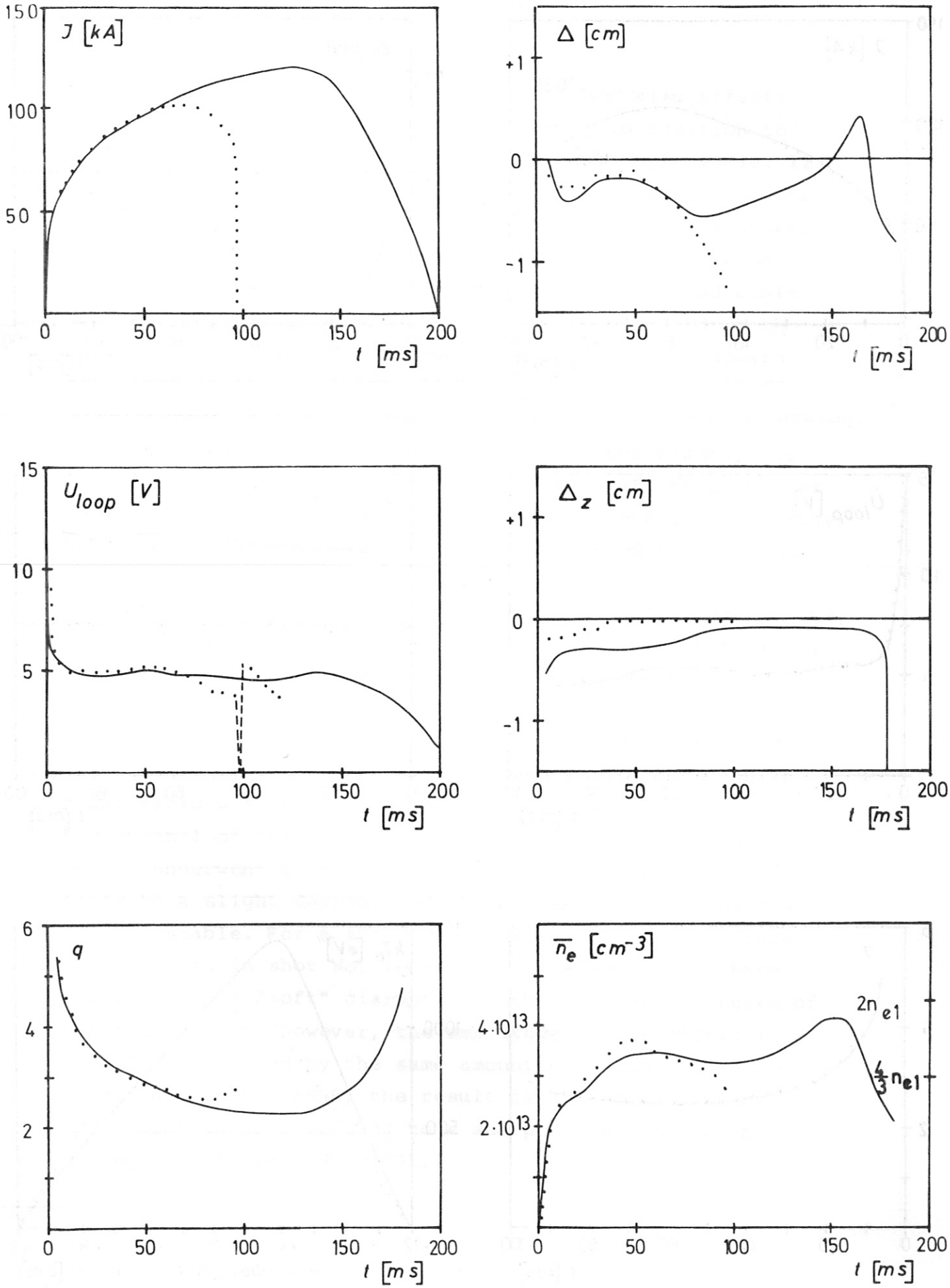

Fig.11. Shots No.1654 and No.1655 with and without premagnetized iron core respectively. Programmed vertical field. B_v = 28 kG.

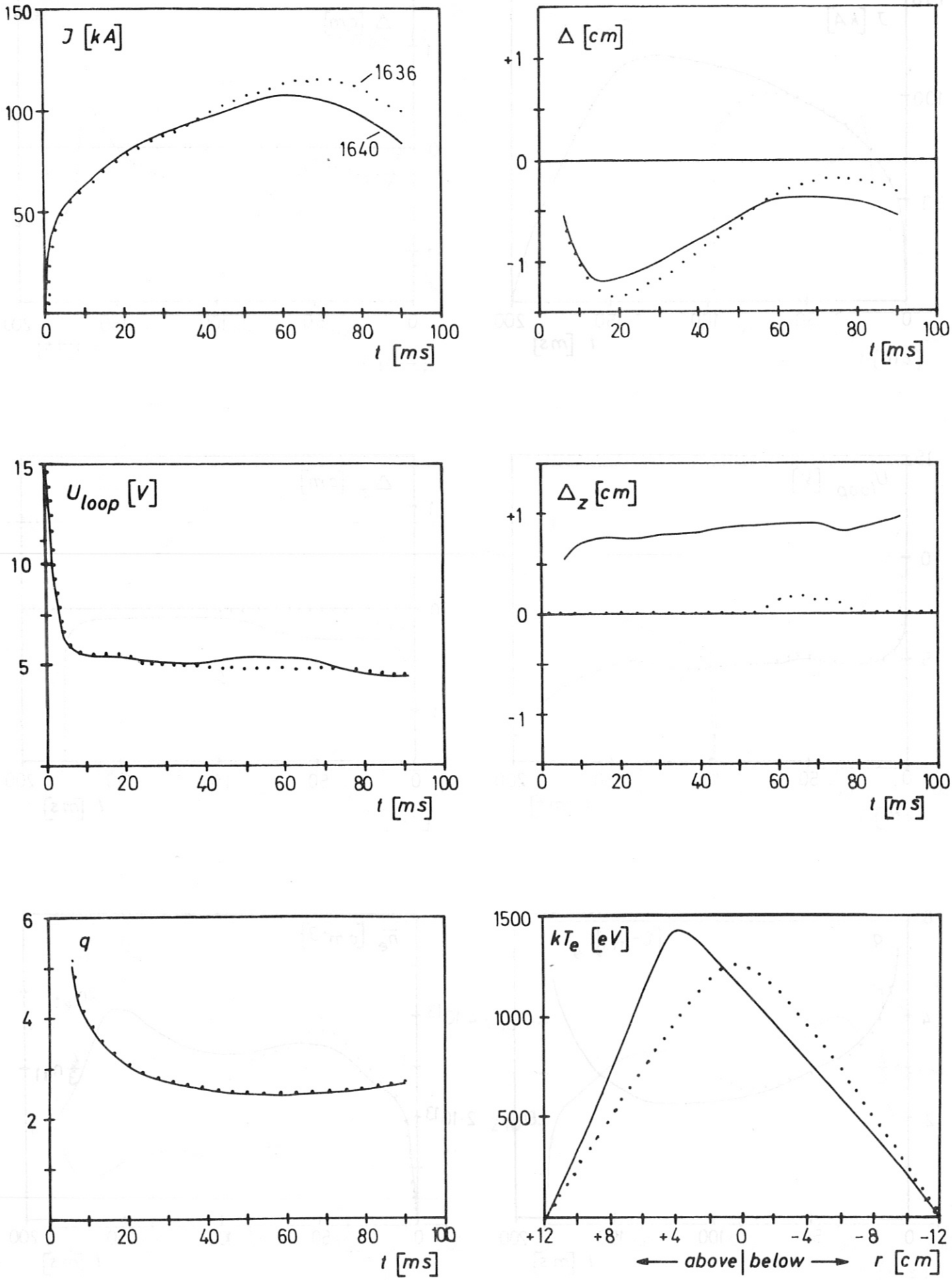

Fig. 12. Shots No.1636 and 1640 with corrected and uncorrected radial field respectively. Programmed vertical field. B_φ = 29,5 kG.

The vertical centering of the plasma column also affects the time variation of the current itself, in addition to the other plasma parameters. This can be seen from Fig. 12, in which two discharges with and without correction of the radial stray magnetic field are compared with one another. The current increases more slowly in the case of the uncorrected radial field. Both discharges were reproducible and vertical temperature profiles were recorded for both cases, these also being presented in Fig. 12. The upward displacement of the plasma column causes a much stronger displacement of the temperature maximun in the same direction. As regards the horizontal displacement of the plasma, the discharges with programmed vertical fields afforded further confirmation of the explanation of the different instability behaviour when the plasma column is displaced outwards and inwards, the preceding figures being cases in point. The programmable power supply of the vertical field windings inside the copper shell also allowed a remarkable experiment, the results of which are presented in Figure 13.

In discharge No. 1884 the plasma column is well centered and stable. In discharge No. 1886 the amplitude of the vertical field was reduced for a short time by a change in one channel of the program generator, and so the plasma column underwent a stronger outward displacement. This leads to a slight decrease of the current, but the plasma remains stable. For a stronger reduction of the amplitude such as that in shot No. 1888 the displacement is greater and leads to a "soft" disruption with a renewed increase of the current. If, however, the amplitude of the vertical field is increased by the same amount by which it was reduced in shot No. 1886, the result is a displacement of the plasma inwards leading to a sharp disruption of the current, as in shot No. 1891.

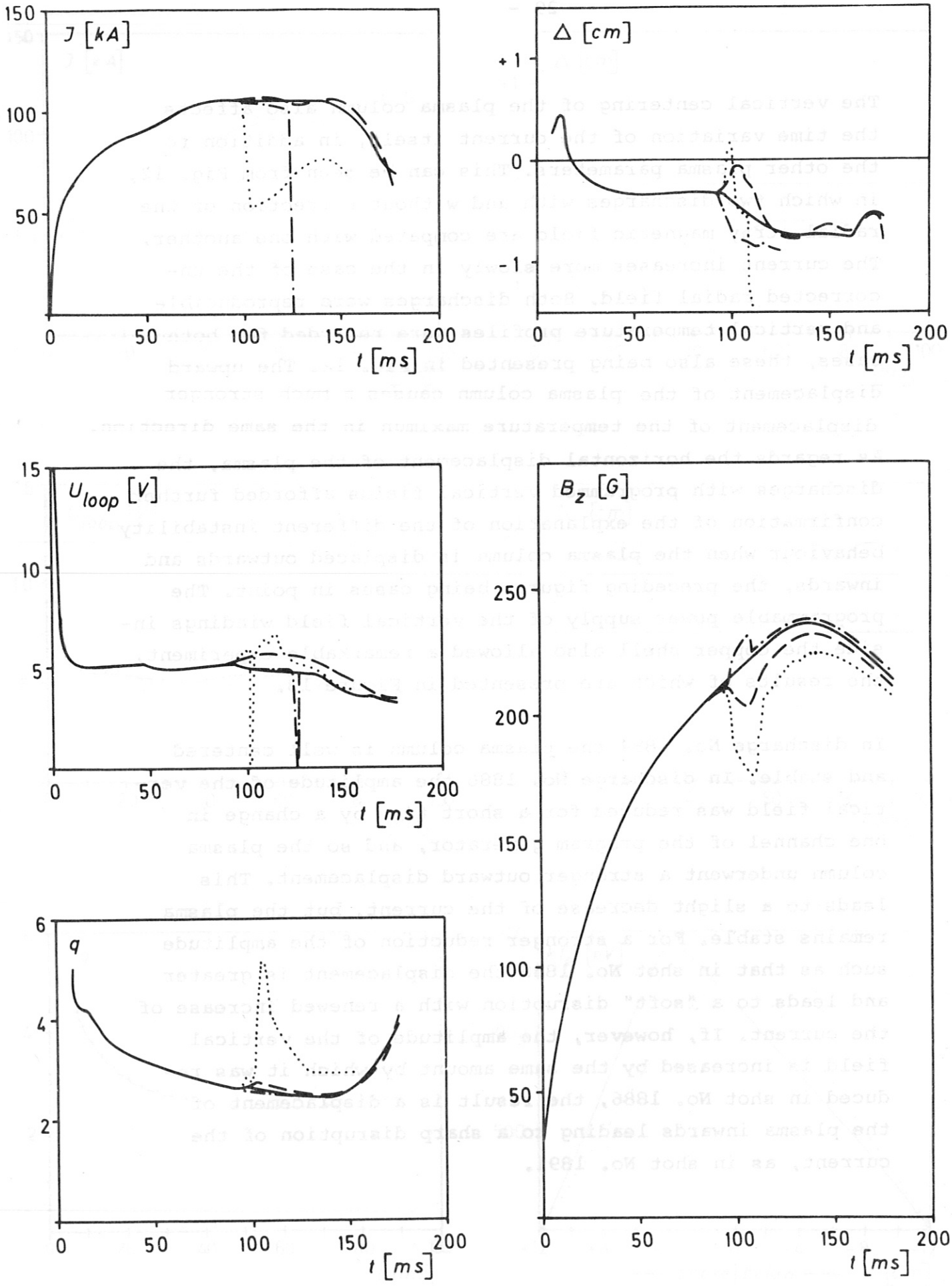

Fig.13. Shots No. 1884 ———, 1886 - - - , 1888 • • • • and 1891 - • - • - with programmed vertical fields. B_φ = 29 kG.

The outcome of this experiment may be regarded as a further, very convincing confirmation of the model advanced in Section III for the different developments of the disruptive instability when the plasma column is displaced outwards or inwards. In any case, it looks as if the disruptive instability could be triggered with predictable results by displacing the plasma column inwards or outwards. It should also be specially mentioned that the characteristics occurring in the case of "spontaneous" instabilities are also observed in the case of "artificially induced" instabilities, namely

- negative voltage spike
- current decrease
- decrease of electron density.

In future experiments it will be attempted with a multichannel transient recorder to perform highly time-resolved investigations of the time developments of as many phenomena as possible - current, loop voltage, displacement signal, displays of further magnetic probes (MHD modes), phase shifts in the channels of the microwave interferometer, etc.

Four channels of the recorder were already in operation during the last few discharges in the period covered by this report. They were used for investigating MHD modes detected with magnetic probes. As in, for example, T 3, modes with $m = 2, 3, 4 \ldots$ were also found here. When $q(a)$ is in the vicinity of an integral value, then modes with $m = q(a)$ predominate. Strong growth of the amplitude was always found before the onset of the disruptive instability; this also applied to the induced current disruptions mentioned

above. The MHD modes m = 2 - 4 also manifested themselves very clearly as noise in the loop voltage. In the discharges in which the current was so large that q values of less than 3 were reached, it was easily possible to observe the times at which q = 4 and q = 3 were crossed. At these times the signals of the microwave interferometer were also affected by noise.

The onset of disruptions at nearly integral q values is probably related to the fact that the MHD mode with mode number m = q has its maximum amplitude when q is integral. However, this condition alone is not sufficient for the production of a disruptive instability. The experiments described above have shown that crossing of integral values of $q > 3$ with increasing current is possible if the plasma column is centered sufficiently well; the maximum permissible value of $|\Delta|$ tends to decrease with decreasing q. This reinforces the view - at least for the q regime covered by the experiments - that enhanced interaction of the plasma with the limiter plays an important role in the onset of the disruptive instability. The mechanism of that interaction is unknown as yet. A possible explanation is the formation of magnetic islands due to the MHD modes /5/. For integral q values such islands are created close to the edge of the limiter. One would expect that in this case even a small displacement of the plasma column should have a strong influence on the island structure. This explanation is supported by the results of the experiments with superimposed helical fields in Pulsator I /6/, where islands are also created by the stellarator windings.

If the discharge is well centered according to the magnetic probes, then the electron density and temperature are also symmetric, to a good approximation, about the minor torus axis. An example of T_e was shown in Figure 12; an example of n_e is shown in Figure 14, which, like Figure 7, plots the average electron density at various times for discharge No. 1079 represented in Figure 9.

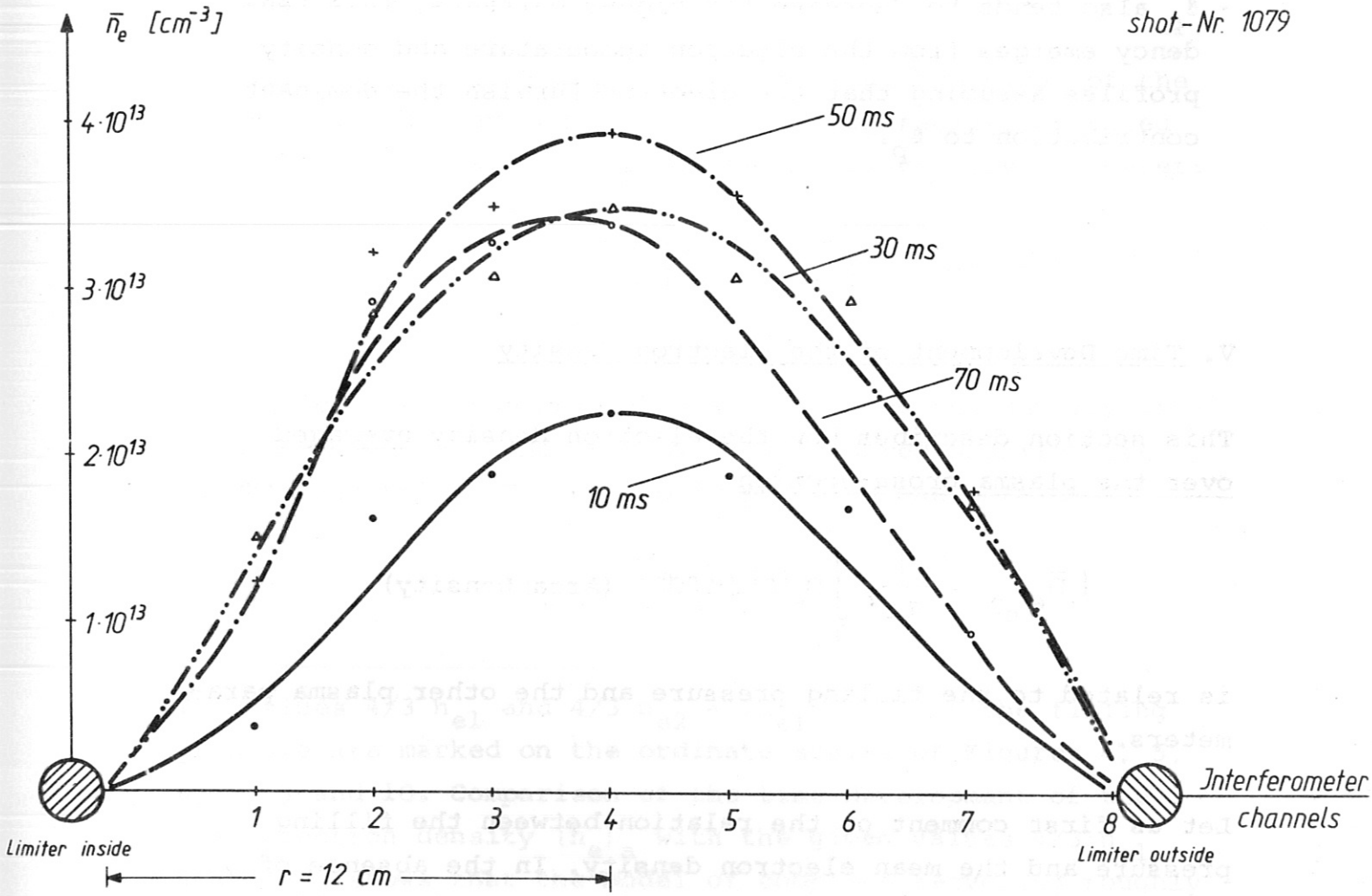

Fig. 14 Shot No. 1079 (cf. Fig. 9). Profiles of the electron density averaged over the microwave path lengths.

Finally, the behaviour of the quantity $\beta_p + l_i/2$ is briefly discussed. As comparison of the various figures shows, $\beta_p + l_i/2$ tends to decrease for larger currents. According to the results obtained so far this has two causes:

- At lower currents the temperature profiles are bell-shaped with a half-width in radius down to 4 cm, while at higher currents they are wider. If the conductivity distribution behaves accordingly, this leads to a reduction of l_i.

- β_p also tends to decrease for higher currents. This tendency emerges from the electron temperature and density profiles assuming that the electrons furnish the dominant contribution to β_p.

V. Time Development of the electron density

This section describes how the electron density averaged over the plasma cross-section

$$(\bar{n}_e)_{a^2} = \frac{1}{\pi a^2} \int_0^a n_e(r) 2\pi r dr \quad \text{(Area Density)}$$

is related to the filling pressure and the other plasma parameters.

Let us first comment on the relation between the filling pressure and the mean electron density. In the absence of plasma-wall interaction the mean electron density would be expected to rise quickly to the value n_{el}, which is given by complete dissociation and ionization of all H_2 molecules

which were present in the liner volume before ignition of the discharge. The hydrogen from the outer parts of the vacuum vessel would then flow through the pump ports, with a time constant of 0.1 s being given by the cross-section of the pump port. As the total volume of the vacuum system is 1.5 times that of the liner volume, the density should continue to rise slowly from n_{e1} to a maximum of $n_{e2} = 1.5\ n_{e1}$. The time behaviour of the mean electron density would be the same with complete recycling, i. e. if one H atom from the wall were to replenish every ion that is lost.

Figures 4, 5, 6, 8, 9 and 10 show the time behaviour of the electron density <u>averaged over the plasma radius</u>, measured with the horizontal channel of the microwave interferometer:

$$(\bar{n}_e)_a = \frac{1}{a}\int_0^a n_e(r)\,dr. \quad \text{(Line Density)}$$

The ratio of the two mean values depends on the density profile. As Figures 7 and 14 show, the measured profiles are roughly parabolic. For parabolic profiles one obtains

$$(\bar{n}_e)_a = \frac{4}{3}(\bar{n}_e)_{a2} \quad .$$

The values $4/3\ n_{e1}$ and $4/3\ n_{e2} = 2n_{e1}$ given by the filling pressure are marked on the ordinate scales of Figures 4, 5, 6, 8, 9 and 10. Comparison of the time development of the mean electron density $(\bar{n}_e)_a$ with the given values $4/3\ n_{e1}$ and $2\ n_{e1}$ shows that the model of complete recycling roughly describes the actual conditions in some cases, namely those presented in Figures 5, 6, 10 and 11. Strong deviations are observed in Figures 4, 8 and 9. The behaviour in the

case of Figure 4 is typical of the initial phase of operation, in which the vacuum conditions were still unfavourable. In the case of Figures 8 and 9 with particularly low filling densities and relatively high currents the value 2 n_{el} is exceeded at an early stage; the density appears to follow the current, this being ascribed to the emission of hydrogen or wall material.

As to the question what causes the values 4/3 n_{el} and 2 n_{el} given by the filling pressure to be exceeded, a few indirect remarks can be made by examining the effective ion charge number, Z_{eff}, which is defined as

$$Z_{eff} = \frac{\sum n_i Z_i^2}{\sum n_i Z_i} .$$

The mean value of Z_{eff} over the plasma cross-section can be arrived at by comparing the ohmic resistance determined from I and U curves with that predicted by the mean value of the $T_e^{3/2}$ profile assuming Spitzer resistivity.

Available measurements yield typical values between 4 and 10. If it is assumed for the sake of discussion that just one species of impurity ion is present with density n_2 and charge Z_2 in addition to the hydrogen ions with density n_1 one obtains

$$\frac{n_2 Z_2}{n_e} = \frac{Z_{eff} - 1}{Z_2 - 1}$$

$$\frac{n_e}{n_1} = \frac{Z_2 - 1}{Z_2 - Z_{eff}}$$

where $n_2 Z_2 / n_e$ is the fraction of the electrons originating from impurity ions with charge Z_2, and n_e / n_1 is the electron to proton ratio.

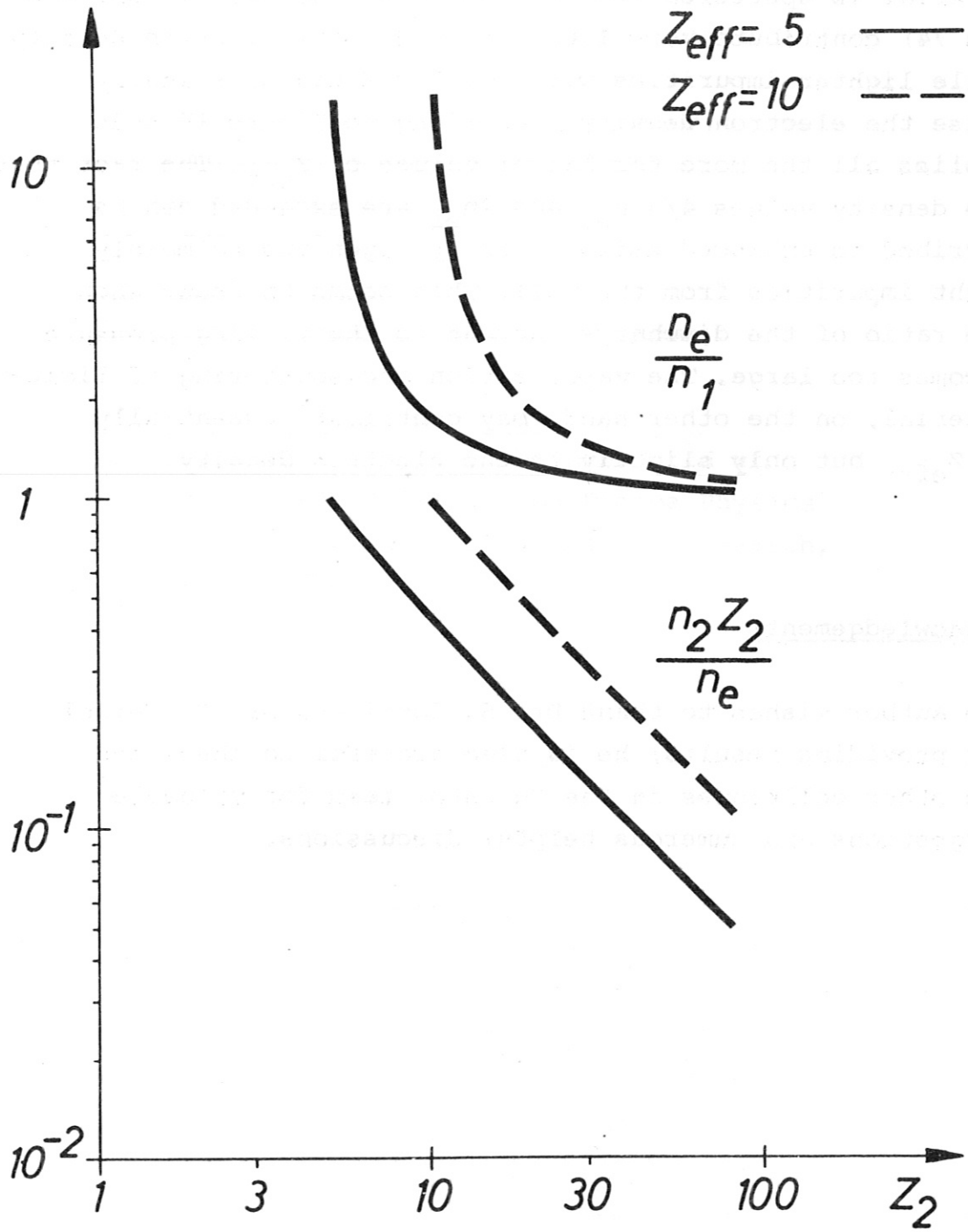

Fig. 15 Ratios of the total electron density n_e to the proton density n_1, and the impurity electron density $n_2 Z_2$ to n_e, plotted as a function of the impurity ion charge Z_2 according to the model given in the text.

In Fig. 15 $n_2 Z_2/n_e$ and n_e/n_1 are plotted as functions of Z_2 for $Z_{eff} = 5$ and $Z_{eff} = 10$. This shows that ions of high charge number such as are mostly expected when limiter material is sputtered (Mo has the atomic number 42, while W has 74) contribute very little to the total electron density, while lighter impurities with smaller Z can drastically raise the electron density. According to Figure 15 this applies all the more for larger values of Z_{eff}. The fact that the density values $4/3\ n_{el}$ and $2n_{el}$ are exceeded can be ascribed to enhanced emission of hydrogen and to mainly light impurities from the wall. This seems to occur when the ratio of the discharge current to the filling pressure becomes too large. The vaporization and sputtering of limiter material, on the other hand, may contribute essentially to Z_{eff}, but only slightly to the electron density.

Acknowledgements

The author wishes to thank Dr. S. Corti and Dr. D. Meisel for providing results; he is also grateful to these and the other colleagues in the Pulsator team for valuable suggestions and numerous helpful discussions.

References

/1/ IPP Garching, annual report 1972

/2/ D. Meisel, IPP report III/15 (1974)

/3/ V.S. Mukhovatov, V.D. Shafranov, Nuclear Fusion 11, 605 (1971)

/4/ IPP Garching, annual report 1973

/5/ P. Chrisman, D. Clarke, J. Rome, ORNL-TM-4501

/6/ F. Karger et al, to be presented at the Fifth Conference on Plasma Physics and Controlled Nuclear Fusion Research, Tokyo 1974